

# AdaptSim: Task-Driven Simulation Adaptation for Sim-to-Real Transfer

Allen Z. Ren\* Hongkai Dai<sup>†</sup> Benjamin Burchfiel<sup>†</sup> Anirudha Majumdar\*  
\* Princeton University <sup>†</sup> Toyota Research Institute

**Abstract**—Simulation parameter settings such as contact models and object geometry approximations are critical to training robust robotic policies capable of transferring from simulation to real-world deployment. Previous approaches typically handcraft distributions over such parameters (domain randomization), or identify parameters that best match the dynamics of the real environment (system identification). However, there is often an *irreducible gap* between simulation and reality: attempting to match the dynamics between simulation and reality across all states and tasks may be infeasible and may not lead to policies that perform well in reality for a specific task. Addressing this issue, we propose AdaptSim, a new *task-driven* adaptation framework for sim-to-real transfer that aims to optimize task performance in target (real) environments — instead of matching dynamics between simulation and reality. First, we meta-learn an adaptation policy in simulation using reinforcement learning for adjusting the simulation parameter distribution based on the current policy’s performance in a target environment. We then perform iterative real-world adaptation by inferring new simulation parameter distributions for policy training, using a small amount of real data. We perform experiments in three robotic tasks: (1) swing-up of linearized double pendulum, (2) dynamic table-top pushing of a bottle, and (3) dynamic scooping of food pieces with a spatula. Our extensive simulation and hardware experiments demonstrate AdaptSim achieving 1-3x asymptotic performance and  $\sim 2x$  real data efficiency when adapting to different environments, compared to methods based on Sys-ID and directly training the task policy in target environments.<sup>1</sup>

## I. INTRODUCTION

Learning robust policies for real-world manipulation tasks typically requires a substantial amount of training data. Since using real data exclusively can be very expensive or even infeasible, we often resort to training mostly in simulation. This raises the question: how should we specify simulation parameters to maximize performance in the real world while minimizing the amount of real-world data we require?

A popular method among the robotics community is to perform *domain randomization*: train a policy using a wide range of different simulation parameters in the hope that the policy can thus handle possible real-world variations in dynamics or observations. This approach has enabled some of the most prominent successes in sim-to-real transfer of robotic policies [2, 16, 23, 26]. However, the trained policy may achieve good *average* performance, but perform poorly in a particular real environment. Addressing this issue, there has been work in performing system identification (Sys-ID) for providing a point or a distributional estimate of parameters that best matches the robot or environment dynamics exhibited

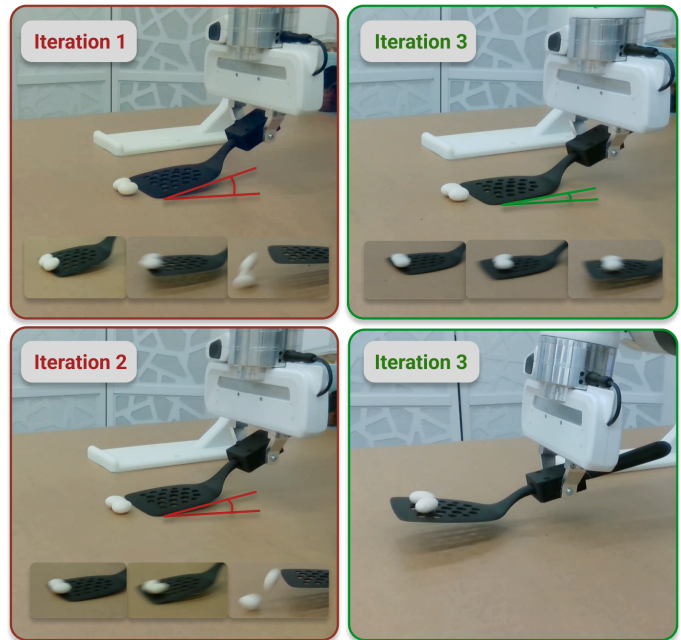


Fig. 1: AdaptSim iteratively infers a better simulation parameter distribution for training the task policy in simulation based on real trajectory observations of executing a task policy. When dynamically scooping up chocolate raisins, the updated task policy learns to use smaller initial pitch angle of the spatula from the table, such that the pieces do not bounce off after contact.

in real-world data. This estimation can be performed using either a single iteration [25] or multiple ones [34]. These *adaptive* domain randomization techniques allow training policies suited to specific target environments.

While simple objects such as a box and its properties like the inertia can be well-modeled, there is a substantial amount of “irreducible” sim-to-real gap in many settings such as contact-rich manipulation tasks. Consider the task of using a cooking spatula to dynamically scoop up small pieces of food from a table (Fig. 1). The exact object geometry of the pieces and spatula is difficult to specify, deformation such as the spatula bending against the table is not yet maturely implemented in simulators, and contact models such as point contact have been known to poorly approximate the complex real-world contact behavior [28] in these settings. In this case, real environments are out-of-domain (OOD) from simulation, and performing Sys-ID of simulation parameters might fail to train a useful policy for the real world due to this inherent irreducible gap.

In this work we take a *task-driven* approach: instead of trying to align the simulation with real-world dynamics, we

<sup>1</sup>video available at <https://youtu.be/p2msMCOFDDg>

focus on finding simulation parameters such that the resulting policy optimizes task performance. Such an approach can lead to policies that achieve high reward in the real world even with an irreducible sim-to-real gap. We consider settings where the robot has access to a simulator between iterations of real-world interactions, allowing it to observe real-world dynamics and update the simulator accordingly with the goal of improving task performance in reality. Additionally, this approach enhances the efficiency of real data usage by identifying only task-relevant simulation parameters and helps trained policies better generalize to OOD (real) environments.

**Statement of Contributions.** We propose *AdaptSim*, an approach for efficient sim-to-real behavior transfer that interleaves simulation learning with real-world exploration. AdaptSim iteratively adapts the simulation parameter distribution used during policy training to maximize performance in a target environment such as reality. The following is a summary of our contributions:

- We propose an adaptation policy that adjusts a simulation parameter distribution based on the current task policy’s performance and behavior in the target environment. Instead of predicting the optimal distribution in one step, the adaptation incrementally changes the distribution through a small number of interactions with the target environment. The adaptation policy is trained using Reinforcement Learning (RL) to maximize the future task reward achieved.
- We propose a two-phase setup where (i) the adaptation policy is first meta-trained to adapt to different simulated target environments (randomly sampled from the entire parameter space in simulation), and (ii) then deployed on the real environment iteratively. We formalize the meta-learning setting by introducing the Simulation-Adaptation Contextual Bandit (SA-CB). In the second phase, the policy uses a small number of interactions with the real environment in order to infer the optimal change of simulation parameter distribution for training a task policy to execute in the next iteration. The same adaptation policy can be re-used for adapting to different real environments.
- We demonstrate our approach achieving 1-3x asymptotic performance and  $\sim 2x$  real data efficiency when adapting to different hardware or simulated OOD environments in three robotic tasks including two that involve contact-rich manipulation, compared to methods based on Sys-ID and directly training the task policy in target environments.

## II. RELATED WORK

Sim-to-real transfer in robotics has been primarily addressed using Domain Randomization (DR) techniques [2, 18, 44, 38, 33, 27] that inject noise in simulation parameters related to visuals, dynamics, and actuations. A comprehensive review can be found in [31]. A straightforward way of designing the simulation parameter setting is to hand-engineer it and keep it fixed throughout the task policy training, which can be sample-inefficient and even hinder policy training [29]. Below we summarize techniques that better adapt to real environments.

**Sys-ID domain adaptation.** Inspired by classical work in Sys-ID [12, 21], there has been a popular line of work identifying simulation parameters that match the robot and environment dynamics in the real environment before task policy training. BayesSim [34] and follow-up work [17, 5] applies Bayesian inference to iteratively search for a posterior distribution of the simulation parameters based on simulation and real-world trajectories. The inference problem has also been formulated using RL to minimize trajectory discrepancies [7]. A different approach [3, 1, 51] learns a residual model of dynamics (often parameterized with a neural network) to match simulation or an ideal physics model with reality. However, all these methods consider relatively well-modeled environment parameterizations such as object mass or friction coefficient during planar contact; Sys-ID approaches have been shown to fail in cases where the simulation does not closely approximate the real world [31, 9]. There is also work that avoids inferring the full dynamics but adapts with a low-dimensional latent representation online [22, 49, 10], but the representation is still trained with regression to match dynamics or simulation parameters. Importantly, the Sys-ID approaches highlighted above are all task-agnostic; this can lead to poor performance when trained task policies are sensitive to mismatches in dynamics between simulation and reality. Chi et al. [9] address the issue by using simulation to predict changes to trajectories from changes in actions as an implicit policy, but it requires the environment to be resettable, while AdaptSim works with randomly initialized object states.

**Task-driven domain adaptation.** AdaptSim better fits within a different line of work that aims to find simulation parameters that maximize the task reward in target environments. Muratore et al. [30] apply Bayesian Optimization (BO) to optimize parameters such as pendulum pole mass and joint damping coefficient in a real pendulum swing-up task. Other work focus on adapting to simulated domains only [47, 50, 37]. One major drawback of these methods is that they require a large number of rollouts in target environments (e.g., 700 in [30]), which is very time-consuming for many tasks requiring human reset. AdaptSim meta-learns adaptation strategies in simulation and requires only a few real rollouts for inference (e.g., 20 in our pushing experiments). Liang et al. [24] apply the same task-driven objective to learn an exploration policy in manipulation tasks, but the task policy is synthesized using estimated simulation parameters via Sys-ID. Jin et al. [19] applies task-driven reduced-order model for dexterous manipulation tasks, but again the model is identified with Sys-ID and no vision-based control is involved. Ren et al. [35] search for adversarial environments (e.g., objects) given the current task performance to robustify the policy, but unlike AdaptSim, the adversarial metric is measured in simulated domain only without real data.

**Learn to search/optimize.** Our work involves learning optimization strategies through meta-learning across a distribution of relevant problems, allowing for customization to the specific setting and increased sample efficiency [13, 48]. Chen et al. [8] meta-learns an RNN optimizer for black-box optimization.

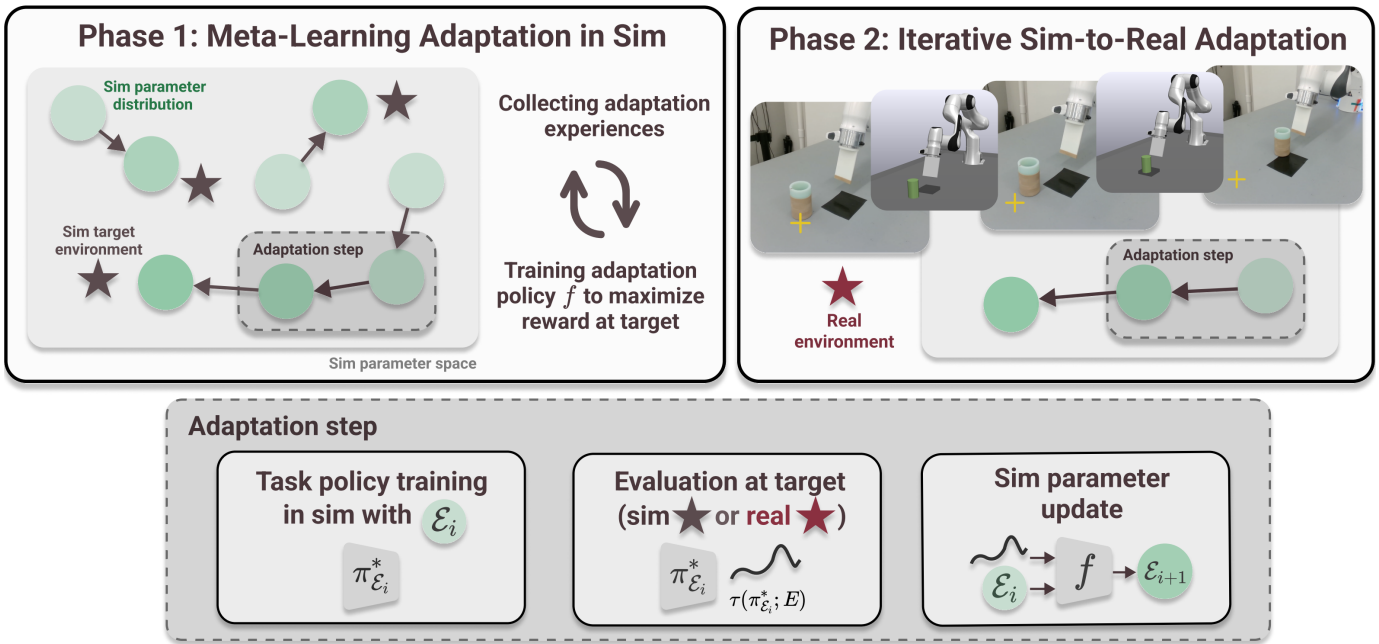


Fig. 2: AdaptSim consists of two phases: (1) meta-training an adaptation policy in simulation by maximizing task reward on randomly sampled simulated target environments; (2) iteratively adapting simulation parameter distributions based on real trajectories. In simulation, the adaptation policy  $f : (\mathcal{E}, \tau) \mapsto \Delta_{\mathcal{E}}$  is trained to adjust the current simulation parameter distribution based on the task policy’s trajectory in the target environment; the new distribution is predicted to achieve better task performance in the next iteration. In the real environment, the adaptation policy selects a better simulation parameter distribution using the trained  $f$ , and the task policy is iteratively fine-tuned in simulation. The upper-right illustration shows an example of this process: using only a few real trajectories, the task policy is adapted to push the bottle closer to the target location (yellow cross).

Volpp et al. [46] meta-learns the acquisition function in BO with RL; it is able to learn new exploration strategies for black-box optimization and tuning controller gains in sim-to-real transfer. Meta RL trains the task policy directly to optimize performance in new environments [36, 20, 32] — AdaptSim applies meta RL to optimize simulation parameters instead.

### III. PROBLEM FORMULATION

**Environment.** In simulation, we consider a space  $\Omega$  that parameterizes the environment with quantities such as friction coefficients and dimensions of geometric primitives. Let  $\mathcal{E}$  denote a distribution of simulation parameters with support on  $\Omega$ . We sample an individual environment  $E \in \Omega$  from  $\mathcal{E}$  and we denote a real environment  $E^r$ . Importantly, we do not parameterize the underlying space of  $E^r$ , since it may be arbitrarily complex or impossible to be fully captured by the particular  $\Omega$  available with existing simulators.

**Task Policy.** We denote a task policy  $\pi \in \Pi : \mathcal{O} \rightarrow \mathcal{A}$  that maps the robot’s observation  $o_t$  to action  $a_t$ . The observation space  $\mathcal{O}$  and the action space  $\mathcal{A}$  depend on the task considered.

**Trajectory.** Running the task policy in a particular environment results in a state-action trajectory  $\tau(\pi; E) : [0, T] \times \Pi \times \mathcal{E} \rightarrow \mathcal{S} \times \mathcal{A}$  with time horizon  $T$ . The trajectory is also subject to an initial state distribution. We specify tasks for the robot using a reward function, and let  $R(\tau) \in [0, 1]$  denote the normalized cumulative reward accrued by a trajectory. We let  $R(\pi; E)$  denote the reward of running the task policy  $\pi$  in the environment  $E$ , in expectation over the initial state distribution.

**Goal.** Our eventual goal is to find a task policy that maximizes the task performance in a real environment  $E^r$ :

$$\sup_{\pi} R(\pi; E^r). \quad (1)$$

In this work, we use the distribution  $\mathcal{E}$  of simulation parameters to compactly parameterize the policy  $\pi$ . This leads to the following bi-level optimization objective:

$$\sup_{\mathcal{E}} R(\pi_{\mathcal{E}}^*; E^r), \text{ where } \pi_{\mathcal{E}}^* := \sup_{\pi} \mathbb{E}_{E \sim \mathcal{E}} [R(\pi; E)], \quad (2)$$

the optimal task policy for the training distribution  $\mathcal{E}$ . Performing the outer level of (2) requires interactions with  $E^r$  (the real world); we allow a small budget of such interactions. We emphasize that the objective above identifies the optimal distribution of simulation parameters for maximizing task performance, unlike objectives that attempt to match the dynamics between simulation and reality.

### IV. APPROACH

#### A. Overview

One way to solve (2) is to perform blackbox optimization on  $\mathcal{E}$  by evaluating  $R(\pi_{\mathcal{E}}^*; E^r)$  [30]. However, this would require a large budget of real trajectories, which is time- and effort-consuming. AdaptSim instead iteratively *infers* simulation parameters that improve task performance by interacting with the real environment a small number of times. The inference is performed with an “adaptation” policy  $f : (\mathcal{E}, \tau) \mapsto \Delta_{\mathcal{E}}$  that adjusts the current simulation parameter distribution  $\mathcal{E}$  by  $\Delta_{\mathcal{E}}$

based on  $\tau(\pi_{\mathcal{E}}^*; E^r)$ , the trajectory of the trained task policy in the real environment.

This approach can be viewed as an iterative adaptation process which predicts optimal parameter distributions for simulation training based on a small number of observed real-world trajectories. Using the scooping domain from Fig. 1 as an example, at each iteration the robot attempts to scoop up pieces of food in the real world, observes the effects of its attempt, and adjusts simulation parameters before updating its task policy in simulation.

To eventually achieve adaptation in the real environment, AdaptSim consists of two phases (Fig. 2):

- 1) **Meta-learn the adaptation policy in sim:** randomly sample target environments  $E^s \in \Omega$  in simulation, and then train  $f(\mathcal{E}, \tau)$  using RL to maximize task reward in them, by updating the simulation parameter distribution (and the corresponding task policies) in iterations.
- 2) **Iteratively adapt sim parameters with real data:** given a real environment  $E^r$  at deployment time, iteratively infer better simulation parameter distributions for  $E^r$  using the trained  $f$  and a few real trajectories; the task policy is iteratively fine-tuned in simulation to improve task reward with the updated parameter distribution.

### B. Phase 1: meta-learning the adaptation policy in sim

In order to correctly infer improved simulation parameters for an unseen real environment at test time, we first train the adaptation policy to infer better parameters for many simulated target environments. This phase happens entirely in simulation. Formally, we model the problem as a partially-observable contextual bandit [6]:

**Definition 1:** A Simulation-Adaptation Contextual Bandit (SA-CB) is specified by a tuple of  $(\Omega, \mathcal{T}, \mathcal{P}, R)$ , where

- $\Omega$  is the space of contexts. Each context corresponds to a simulated target environment  $E^s$ ; the context is not directly observable.
- $\mathcal{T}$  is the space of partial observations of the context. Each observation corresponds to a trajectory observed by running the task policy in a given context.
- $\mathcal{P}$  is the space of actions. An action corresponds to a choice of the simulation parameter distribution  $\mathcal{E}$ .
- $R$  is the reward associated with choosing an action in a particular context (*i.e.*, the reward  $R(\pi_{\mathcal{E}}^*; E^s)$  of the task policy  $\pi_{\mathcal{E}}^*$  trained with some simulation parameter distribution  $\mathcal{E}$  when deployed in the target environment).

It may be difficult to infer the optimal  $\mathcal{E} \in \mathcal{P}$  using a single iteration of interactions with the target environment — if the current task policy fails badly in the target environment, the interaction may reveal little information. Thus, we iteratively apply incremental changes to  $\mathcal{E}$ , with the parameter distribution initialized as  $\mathcal{E}_{i=0}$ . Solving the SA-CB (using techniques that we detail below), we meta-learn an adaptation policy

$f(\mathcal{E}, \tau)$  to maximize:

$$\mathbb{E}_{E^s \sim \mathcal{U}_{\Omega}} \mathbb{E}_{\mathcal{E}_0 \sim \mathcal{U}_{\mathcal{P}}} \sum_{i=0}^I \gamma^i R(\pi_{\mathcal{E}_i}^*; E^s), \quad (3)$$

where  $\mathcal{E}_{i+1} = \mathcal{E}_i + \Delta_{\mathcal{E}_i}$ ,

$$\Delta_{\mathcal{E}_i} = f(\mathcal{E}_i, \tau(\pi_{\mathcal{E}_i}^*; E^s)),$$

and  $\mathcal{U}_{\Omega}$  and  $\mathcal{U}_{\mathcal{P}}$  are uniform distributions over  $\Omega$  and  $\mathcal{P}$  respectively, and  $\gamma < 1$  is the discount factor. This is the expected discounted sum of task rewards over multiple interactions from  $i = 0$  to the adaptation horizon  $I$ , over random sampling of simulated target environment and initial simulation parameter distribution.

In practice, we are only concerned with the reward if it reaches some minimum threshold — a bad task policy is not useful. Thus we use a sparse-reward version of Eq. (3),

$$\mathbb{E}_{E^s \sim \mathcal{U}_{\Omega}} \mathbb{E}_{\mathcal{E}_0 \sim \mathcal{U}_{\mathcal{P}}} \sum_{i=0}^I \gamma^i \mathbb{1}(R(\pi_{\mathcal{E}_i}^*; E^s) \geq \bar{R}) R(\pi_{\mathcal{E}_i}^*; E^s), \quad (4)$$

where  $\mathbb{1}(\cdot)$  is the indicator function and  $\bar{R}$  is the sparse-reward threshold. Using a sparse reward also discourages the adaptation policy from being myopic and getting trapped at a sub-optimal solution, especially since we use a relatively small  $I$  (*e.g.*, 5-10) in order to minimize the amount of real data, and use a small discount factor  $\gamma$  ( $= 0.9$ ).

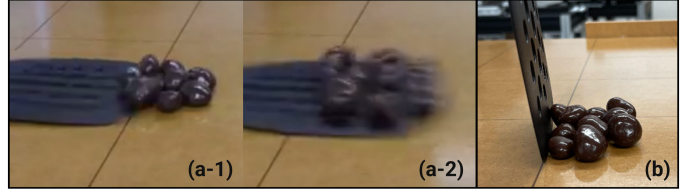


Fig. 3: AdaptSim uses task-policy trajectories that better reveal task-relevant information such as scooping dynamics under fast contact (a-1,2), while simply pushing around the pieces fails to capture it (b).

**Task-policy trajectory as observation.** We have chosen the task policy  $\pi_{\mathcal{E}}^*$  to generate the trajectory observations used by the adaptation policy. While Sys-ID approaches use arbitrary policies or ones that generate the most “informative” trajectories in terms of dynamics [40], they might not be the most informative in terms of revealing optimal parameters for task policy training. Our intuition is that policies that are trained to maximize the task reward are more appropriate since they better reveal the task-relevant information of the target environment. In the scooping task, the robot needs to attempt to scoop up the pieces so it can learn about the effect of the environment on the task (*e.g.*, a piece with a flat bottom is generally harder to scoop). Simply pushing the pieces around does not exhibit the behavior of the pieces under fast contact (Fig. 3).

**Training the adaptation policy using RL.** We apply reinforcement learning (RL) to train the adaptation policy to maximize Eq. (4). In simulation, we collect  $K$  “adaptation trajectories”  $\{(\mathcal{E}_i, \Delta_{\mathcal{E}_i}, R(\pi_{\mathcal{E}_i}^*; E^s), \tau(\pi_{\mathcal{E}_i}^*; E^s))\}_{i=0}^I$ , whose steps are saved in a replay buffer  $\mathcal{S}_f$ . Since each step involves training the corresponding task policy  $\pi_{\mathcal{E}_i}^*$ , which can be

expensive, we apply off-policy Double Q-Learning [45] for sample efficiency. Using this, the adaptation policy outputs the greedy action of a parameterized Q function,  $f(\mathcal{E}, \tau) = \arg \max_{\Delta_{\mathcal{E}}} Q(\mathcal{E}, \tau; \Delta_{\mathcal{E}})$ . We use  $\epsilon$ -greedy exploration (at each step,  $\epsilon$  probability of sampling a random action instead of  $f(\mathcal{E}, \tau)$ ), with  $\epsilon$  initialized at 1 and gradually annealed to 0.

This constitutes the first phase of AdaptSim. Algorithm 1 details the steps for collecting adaptation trajectories in the inner loop (Line 4-15) and meta-learning the adaptation policy. We save all distributions (and their corresponding task policies, omitted in notations for convenience) in a set  $S_{\mathcal{E}}$ , which are used again in the second phase. Training the task policy for each  $\mathcal{E}$  is the most computationally heavy component of Algorithm 1; in Sec. V-C we explain the heuristics applied to allow re-using task policies between  $\mathcal{E}$  that are close to each other in order to improve computational efficiency.

---

**Algorithm 1** Meta-learning the adaptation policy in sim

---

**Require:**  $(\Omega, \mathcal{T}, \mathcal{P}, R)$ , SA-CB  
**Require:**  $S_f = \emptyset$ , replay buffer  
**Require:**  $S_{\mathcal{E}} = \emptyset$ , set of all simulation parameter distributions (and their task policies) used

- 1: Initialize  $\epsilon \leftarrow 1$
- 2: **for**  $k \leftarrow 0$  to  $K$  **do**
- 3:   Sample target  $E^s \sim \mathcal{U}_{\Omega}$  and  $\mathcal{E}_{i=0} \sim \mathcal{U}_{\mathcal{P}}$
- 4:   **for**  $i \leftarrow 0$  to  $I$  **do**
- 5:     Train task policy  $\pi_{\mathcal{E}_i}^*$  with heuristics in Sec. V-C
- 6:     Collect  $\tau(\pi_{\mathcal{E}_i}^*; E^s)$  and  $R(\pi_{\mathcal{E}_i}^*; E^s)$
- 7:     **if**  $\text{rand}() < \epsilon$  **then**
- 8:       Choose a random  $\Delta_{\mathcal{E}_i}$
- 9:     **else**
- 10:        $\Delta_{\mathcal{E}_i} = f(\mathcal{E}_i, \tau(\cdot; \cdot))$
- 11:     **end if**
- 12:     Update  $\mathcal{E}_{i+1} \leftarrow \mathcal{E}_i + \Delta_{\mathcal{E}_i}$
- 13:     Add  $(\mathcal{E}_i, \Delta_{\mathcal{E}_i}, \tau(\cdot; \cdot), R(\cdot; \cdot))$  to  $S_f$
- 14:     Add  $\mathcal{E}_i$  (and  $\pi_{\mathcal{E}_i}^*$ ) to  $S_{\mathcal{E}}$
- 15:   **end for**
- 16:   Train  $f$  using Double Q-Learning and  $S_f$
- 17:   Anneal  $\epsilon$  towards 0
- 18: **end for**
- 19: **return**  $f, S_{\mathcal{E}}$

---

*C. Phase 2: iteratively adapt sim parameters with real data*

After meta-training the adaptation policy to find good task policies for a diverse set of target environments in simulation, we can apply it for inference and perform adaptation for the real environment  $E^r$ . Algorithm 2 details the iterative process. We apply the same adaptation process as the inner loop of Algorithm 1 for  $I^r$  iterations: train the task policy in simulation, evaluate it in the real environment, and infer the change of simulation parameters based on real trajectories. We always apply the greedy action from  $f(\mathcal{E}, \tau)$  (*i.e.*,  $\epsilon = 0$ ).

Since we have already sampled a large set  $S_{\mathcal{E}}$  of parameter distributions and trained their task policies in Phase 1, we may re-use them here. At the beginning of Phase 2, we

sample  $S'_{\mathcal{E}}$ , a set of  $N$  distributions saved in  $S_{\mathcal{E}}$ , as the initial distributions to be adapted independently. Usually we pick  $N = 2$  considering the trade-off between number of real trajectories needed and convergence of task performance (see Appendix C for analysis).

---

**Algorithm 2** Iteratively adapt sim parameters with real data

---

**Require:**  $E^r$ , real environment  
**Require:**  $(\Omega, \mathcal{T}, \mathcal{P}, R)$ , SA-CB  
**Require:**  $f$ , adaptation policy trained in Phase 1  
**Require:**  $S_f$ , set of simulation parameter distributions (and corresponding task policies) from Phase 1

- 1: Sample  $S'_f$  from  $S_f$
- 2: **for**  $i \leftarrow 0$  to  $I^r$  **do**
- 3:   **for**  $\mathcal{E}_i \in S'_f$  **do**
- 4:     Train or fine-tune the task policy  $\pi_{\mathcal{E}_i}^*$  in simulation
- 5:     Collect  $\tau(\pi_{\mathcal{E}_i}^*; E^r)$  and  $R(\pi_{\mathcal{E}_i}^*; E^r)$  in real
- 6:     Update  $\mathcal{E}_{i+1} \leftarrow \mathcal{E}_i + f(\mathcal{E}_i, \tau(\cdot; \cdot))$
- 7:   **end for**
- 8: **end for**
- 9: **return**  $\pi_{\mathcal{E}_i}^*$  with the highest  $R(\cdot; E^r)$

---

## V. IMPLEMENTATION DESIGN CHOICES

Here we elaborate a few design choices, practical considerations, and implementation details of AdaptSim. Additional details are provided in Appendix A.

### A. Trajectory observation

First, we remove the action sequence from the task-policy trajectory and keep the state sequence only. Since the dynamics in real environments can be OOD, in order to achieve similar high-reward states as in simulated environments, the robot would need to use some actions not seen during training (or not seen for the particular state), hindering the adaptation policy to generalize if action sequence were included in the task policy trajectory. We assume that the task-relevant *state* sequence is covered by  $\mathcal{T}$  if the task policy performs reasonably well in the real environment. This choice is also present in the state-only inverse RL literature [11] that addresses train-test dynamics mismatch. See Fig. 11 and related discussions in Sec. VII-D.

We obtain the ground-truth trajectory information in simulation, and estimate it using either point cloud or color contours with a RGB-D camera in the real environment.

### B. Simulation parameter distribution

In this work, we choose the space  $\mathcal{P}$  of possible simulation parameter distributions in the SA-CB to be that of Gaussian distributions with mean bounded within  $\Omega$  (the space of possible simulation parameter settings). The diagonal covariance is fixed and small (typically 1% of the range of the parameter). We choose to adapt only the mean of distributions to limit the search space and thus save the amount of simulation needed for the adaptation policy training.

We also use a fixed step size  $\delta$  for adapting each simulation parameter, ranging from 10% to 15% of the parameter range

depending on the dimension of  $\Omega$ . The set of possible  $\Delta_{\mathcal{E}}$  along each dimension is  $\{\delta, -\delta, 0\}$ . Smaller step size is used for lower dimensional  $\Omega$  for more fine-grained adaptation and task policy training (see Appendix C for sensitivity analysis).

The adaptation policy is parameterized using a Branching Dueling Q-Network [41], which outputs the state-action value of choosing any of the  $\{\delta, -\delta, 0\}$  along each action dimension. It takes in (1) the vector of the mean of current simulation parameter distribution and (2) trajectory observation.

### C. Task policy reuse across parameter distributions

Algorithm 1 requires training the task policy for each  $\mathcal{E}$ , which can be expensive with the two manipulation tasks. Our intuition is that we can share the task policy between parameter distributions of close distance, with the following heuristics:

- Record the total budget (*i.e.*, number of trajectories), and  $j$ , the number of simulation parameter distributions that a task policy has been trained with.
- Define distance between two parameter distribution  $D(\cdot, \cdot)$  such as L2 distance between the mean. If  $\mathcal{E}_i$  is within a threshold  $\bar{D}$  from a previously seen distribution, re-use the task policy. If the policy is already trained with  $M_{\max}$  budget total, do not train again; otherwise train with  $\max(M_{\min}, \alpha^{j-1}M)$  budget, where  $\alpha < 1$  and  $M$  is the budget for training the policy for the first time.
- If the nearby parameter distribution re-uses a task policy, do not re-use the same policy again. This prevents the same task policy being used for too many  $\mathcal{E}$ .

**Remark 1:** re-using task policies between parameter distributions makes the reward  $R$  depend on the adaptation history, as  $\pi_{\mathcal{E}}^*$  depends on previous  $\mathcal{E}$  that are used for training. We choose not to model this history dependency in  $f$ , as the reward should be largely dominated by the current  $\mathcal{E}$ .

## VI. TASKS

We evaluate the effectiveness of AdaptSim across multiple OOD simulated and real environments described below. More details of the task policy training and simulation setup can be found in Appendix B.

### A. Swing-up of a linearized double pendulum

This is a classic control task where the goal is to swing up a simple double pendulum with two actuated joints at one end of the two links and two point masses concentrated at the other end. We consider the dynamics linearized around the state where the pendulum is at the top, and thus we can solve the optimal policy exactly using Linear Quadratic Regulator (LQR) [42] for a particular set of simulation parameters (*i.e.*, a Dirac delta distribution). The task cost (reward) function is defined with the standard quadratic state error and actuation penalty. The trajectory observation is evenly spaced points along trajectory of the two joints.

**Simulation setup.** The environment is parameterized with four parameters as shown in Table. I. The length of the two links is fixed. The dynamics is simulated with numerical integration without a dedicated physics simulator. We consider

OOD simulated settings for this task, and do not consider hardware environments.

Notation	Description	Range
$m_1$	mass of point 1	$[1, 2]$
$m_2$	mass of point 2	$[1, 2]$
$b_1$	damping coefficient of joint 1	$[1, 2]$
$b_2$	damping coefficient of joint 2	$[1, 2]$

TABLE I: Simulation parameters and ranges for the pendulum task.

### B. Dynamic table-top pushing of a bottle

In this task the robot needs to dynamically push a bottle to a particular target location on the table (Fig. 4). Since the target can be outside the workspace of the robot, the robot must push objects with high velocity — causing them to slide after a short period of contact. The task policy is trained to map the desired target location to two values: (1) planar pushing angle and (2) robot end-effector speed (see Appendix B for visualization). The task cost (reward) is defined as the distance between the target location and the final location of the bottle. The trajectory observation is either (1) the final 2D position of the bottle only, or (2) evenly spaced points along the 2D trajectory — we consider both representations in the experiments.

Notation	Description	Range
$\mu$	table friction coefficient	$[0.05, 0.2]$
$e$	hydroelastic modulus [28]	$[1e4, 1e6]$
$\mu_p$	patch friction coefficient	$[0.20, 0.80]$
$y_p$	patch lateral location	$[-0.10, 0.10]$

TABLE II: Simulation parameters and ranges for the pushing task.

**Simulation setup.** We employ the Drake physics simulator [43] for its accurate contact mechanics. In this simulated environment, a small patch of the table is simulated with different physics properties, simulating a wet or sticky area on the work surface. Parameter settings for this task are shown in Table II. The hydroelastic modulus is a parameter of the hydroelastic contact model [28] implemented in Drake — it roughly simulates how “soft” the contact is between the objects, with lower values being softer.

**Real setup.** Two 3D-printed bottles (Fig. 5, Heavy and Light) with the same dimensions but different materials and masses are used. They both have the same low-friction tape at the bottom to allow longer sliding distance. With an idealized model, the sliding distance should only depend on the contact surface but not the mass — which is the case in simulation — but in real experiments, we find the two bottles consistently travel different distances. Additionally, Heavy tends to rotate slightly despite being pushed straight due to a slightly uneven bottom surface. This type of unmodeled effect exemplifies the irreducible sim-to-real gap: no possible setting of the exposed simulation parameters can perfectly reconcile this behavior with that of the simulation. We also adhere a small piece of high-friction Neoprene rubber to the table. This patch will significantly decelerate the sliding bottle and further complicate the real-world task dynamics.

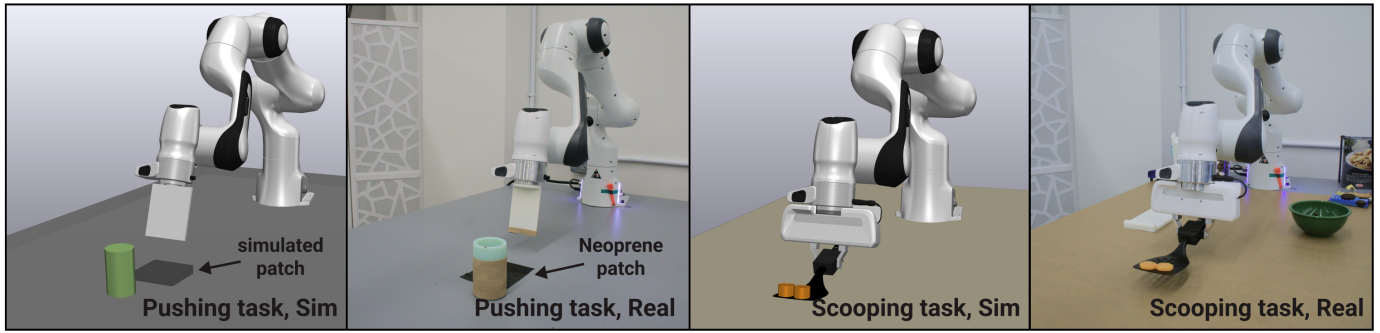


Fig. 4: Setup of the dynamic pushing and dynamic scooping tasks in both simulation and reality.

### C. Dynamic scooping of food pieces with a spatula

In this task the robot needs to use a cooking spatula to scoop up small food pieces on the table (Fig. 4). Unlike previous work where the piece can be scooped against some object with quasi-static motion (e.g., using a stopper [14] or inside a bowl [39]), here the robot has to use the inertial effect from fast acceleration of the spatula to scoop up the pieces dynamically, which is much more challenging and requires intricate planning of the scooping trajectory. We have noticed that humans cannot complete the task consistently without a few trials to practice.

The task policy is trained to map the initial positions of the food pieces to three values that parameterize the whole scooping trajectory: (1) initial distance of the spatula from the pieces, (2) initial pitch angle of the spatula from the table, and (3) the timestep when the robot starts to lift up the spatula and pitch backwards (see Appendix B for details). The task reward is defined as the ratio of food pieces on the spatula at the end of the action. The trajectory observation is evenly spaced points along 2D trajectories of the food pieces, except for more sampling around the first contact between the spatula and a piece.

**Simulation setup.** We again use the Drake simulator. The parameter settings are shown in Table III. The food piece geometry is either an ellipsoid or a cylinder with fixed length/width but varying in height.

Notation	Description	Range
$\mu$	friction coefficient	[0.25, 0.4]
$e$	hydroelastic modulus	[1e4, 5e5]
$g$	food piece geometry	{ellipsoid, cylinder}
$h$	food piece height	[1.5cm, 2.5cm]

TABLE III: Simulation parameters and ranges for the scooping task.

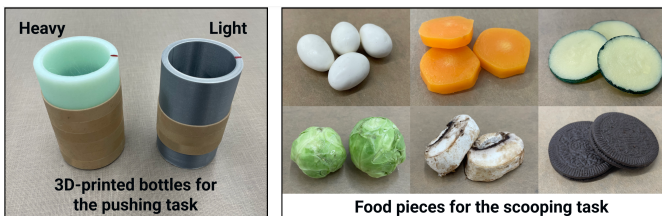


Fig. 5: Real objects used in the pushing and scooping tasks.

**Real setup.** Six different kinds of food pieces are used (Fig. 5): (1) chocolate raisin, (2) (fake, rubber-like) sliced carrot, (3) (fake, rigid) sliced cucumber, (4) raw Brussels sprout, (5) raw sliced mushroom, and (6) Oreo cookie. They cover different shapes from being round, ellipsoidal, to roughly cylindrical, and also have different amounts of deformation and friction.

## VII. EXPERIMENTS

Through extensive adaptation experiments and additional studies in both simulated and real environments, we investigate the following key questions:

- Q1 - Asymptotic Performance: Does AdaptSim improve asymptotic task performance compared to Sys-ID and other baselines when adapting to real environments and OOD simulated environments?
- Q2 - Data Efficiency: Does AdaptSim improve task performance in a data-limited regime compared to Sys-ID and other baselines when adapting to real environments and OOD simulated environments?
- Q3 - Parameter Sensitivity: How does the choice of the simulation parameter space  $\Omega$  affect the task performance in target environments for AdaptSim and baselines?

### A. Baselines

We compare AdaptSim with the following baselines. Each method receives the same data budget for interactions with the target (real-world) domain except where otherwise noted.

- **Uniform domain randomization (UDR).** Train a single task policy to optimize the average task reward over sampled environments from  $\mathcal{U}_\Omega$ . No real-world data is used.
- **UDR+Target.** Fine-tune the task policy trained with UDR with real data. For fine-tuning stability, we fill half of the batch in each gradient update with simulation data.
- **SysID-Bayes [34].** Iteratively infer the simulation parameter distribution based on real trajectories to match dynamics in simulation and reality. The task policy is fine-tuned with the new distribution at each iteration. The implementation is based on open-sourced code [4].
- **SysID-Point.** Similar to SysID-Bayes but infer a point estimate of the simulation parameter instead of a distributional one. We include this baseline since in some settings randomizing simulation parameters with a distribution can negatively impact task policy training.

Method	Double Pendulum Swing-Up					Bottle Pushing					Food Scooping				
	WD	OOD-1	OOD-2	OOD-3	OOD-4	WD	OOD-1	OOD-2	OOD-3	OOD-4	WD	OOD-1	OOD-2	OOD-3	OOD-4
AdaptSim	<b>0.98</b>	<b>0.96</b>	<b>0.95</b>	<b>0.95</b>	<b>0.98</b>	0.95	0.87	<b>0.73</b>	0.86	0.77	<b>1.00</b>	0.64	<b>1.00</b>	<b>1.00</b>	<b>0.55</b>
AdaptSim-State	0.94	<b>0.96</b>	0.93	<b>0.95</b>	0.97	0.96	<b>0.89</b>	0.72	<b>0.88</b>	<b>0.79</b>	-	-	-	-	-
SysID-Bayes [34]	0.85	0.76	0.79	0.23	0.96	<b>0.98</b>	0.80	0.65	0.81	<b>0.79</b>	0.90	<b>0.66</b>	0.81	<b>1.00</b>	0.36
SysID-Bayes-State	0.95	0.87	0.57	0.78	0.93	0.97	0.83	0.68	0.82	<b>0.79</b>	-	-	-	-	-
SysID-Point	0.95	0.60	0.73	0.39	0.76	0.94	0.84	0.68	0.85	0.78	0.94	0.63	0.90	<b>1.00</b>	0.42
SysID-Point-State	0.93	0.90	0.73	0.66	0.94	0.95	0.82	0.67	0.83	0.78	-	-	-	-	-
UDR	-	-	-	-	-	0.68	0.65	0.61	0.67	0.58	0.65	0.22	0.43	0.55	0.12
UDR+Target	-	-	-	-	-	0.78	0.73	0.66	0.71	0.70	0.61	0.31	0.49	0.60	0.21
LearnInTarget	-	-	-	-	-	0.91	0.75	0.66	0.74	0.71	0.03	0.00	0.25	0.26	0.03

TABLE IV: Best average reward achieved over adaptation horizons at different WD and OOD **simulated** target environment in the three tasks. For the pendulum task, the values are normalized in  $[0, 1]$  using the reward achieved by UDR (lower bound) and by using the best possible parameters within  $\Omega$  (upper bound, estimated with exhaustive sampling). For the pushing task, the values are normalized with 20cm as the maximum error, which is the range of possible goal locations in the forward direction.

- **SysID-Bayes-State** and **SysID-Point-State**. Same as SysID-Bayes and SysID-Point but only use high-reward states of the trajectory, which are states near the top in the pendulum task and the final position of the bottle in the pushing task. We then introduce **AdaptSim-State** as a variant of AdaptSim that uses the same high-reward state as the trajectory observation. This set of baselines is not used in the scooping task since the reward is not well-defined until the end of the trajectory.
- **LearnInTarget**. Directly train a task policy with data in the target environment only by fitting a small neural network that maps action to final reward, without iterative adaptation. The policy then outputs the action with the highest predicted reward. We assign the same total number of trials in the target environment as other methods.

UDR+Target and LearnInTarget are not used in the pendulum task since they are not applicable for the LQR policy class.

### B. Results: task performance with adaptation

To answer Q1, we perform experiments for all baselines adapting to different WD (Within-Domain) and OOD simulated environments and also real environments. WD environments are generated by sampling all simulation parameters within  $\Omega$  of each task, and OOD environments are generated by sampling some parameters outside  $\Omega$  (see Appendix C for details). Table IV shows the adaptation results in the *simulated* target environments in the three tasks. While Sys-ID baselines achieve high reward in WD environments, AdaptSim outperforms Sys-ID baselines in almost all OOD environments.

Next, Fig. 6 shows the average reward achieved at each adaptation iteration in different *real* environments in the pushing and scooping tasks. Generally the performance gap between AdaptSim and Sys-ID baselines is larger in reality, with AdaptSim achieving better performance. In the scooping task, for example, AdaptSim is able to train a task policy for sliced cucumbers with decent performance (60% success rate); the pieces are very thin and difficult to scoop under (Fig. 10). Other baselines fail to scoop up the pieces.

We also notice that using high-reward states as the trajectory observation tends to work better than using all states for Sys-ID baselines in the double pendulum and pushing tasks. This is expected as Sys-ID should now better capture task-relevant dynamics of the environment. However, there is no significant performance difference between AdaptSim and AdaptSim-State — AdaptSim can automatically extract useful features from raw trajectories without requiring additional information.

### C. Results: real data efficiency

To answer Q2, we compare AdaptSim with LearnInTarget and UDR+Target with different number of real data budget. With enough data, LearnInTarget and UDR+Target should achieve high reward in the target environment. We do not compare with Sys-ID baselines here since Sec. VII-B shows they typically fail to achieve the same level of task performance in real environments. In the task of pushing Heavy bottle, Table V shows that AdaptSim achieves a similar level of task performance ( $\sim 0.83$ ) using only 16 trials while LearnInTarget and UDR+Target uses 40. Fine-tuning with real data in UDR+Target is ineffective until the real budget is sufficient and can negatively impact the performance in low data regime (e.g., 4 and 8). This also exemplifies using simulation to amortize data requirements for policy training.

Method	Real data budget							
	0	4	8	16	24	32	40	48
AdaptSim	0.30	0.69	0.80	0.83	0.84	0.84	0.82	0.83
LearnInTarget	0.05	0.04	0.63	0.69	0.76	0.80	0.84	0.83
UDR+Target	0.63	0.56	0.62	0.66	0.68	0.74	0.82	0.82

TABLE V: Normalized reward achieved using different amount of real data in the pushing task with Heavy bottle.

While LearnInTarget and UDR+Target achieve reasonable performance in the pushing task, LearnInTarget achieves low reward on all the food pieces in the scooping task, and UDR+Target does not improve upon the performance of UDR policies. The action space in the scooping task is more

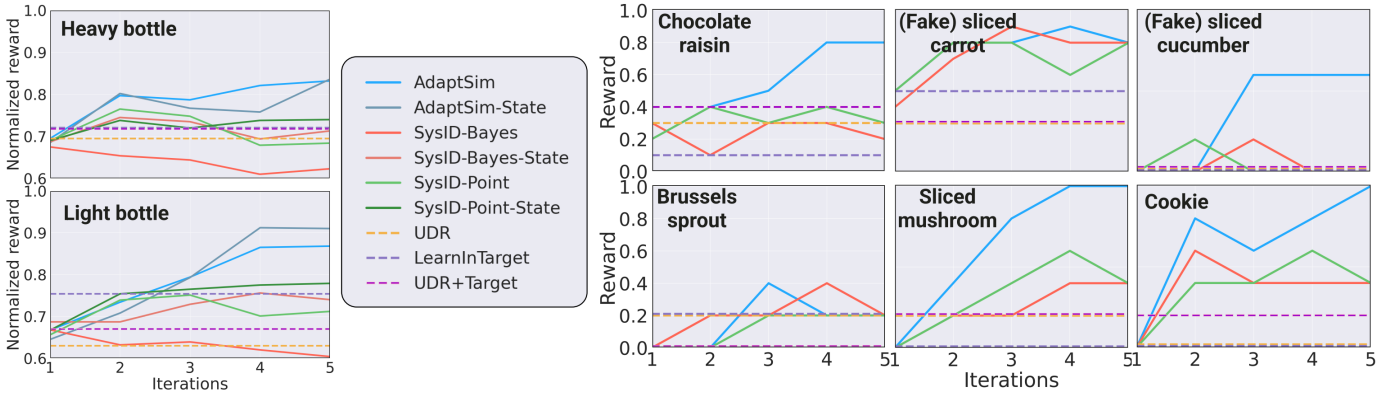


Fig. 6: Reward (averaged over 10 trials in the pushing task and 5 in the scooping task) achieved over adaptation iterations by all methods, in the task of pushing Heavy and Light bottles (left) and scooping up the six different food pieces (see Fig. 5 for images) in real setup.

complex and requires significantly more data to search for or improve task policies. AdaptSim’s adaptation pre-training in simulation considerably amortizes the real data requirement.

#### D. Discussions

**Choice of the simulation parameter space.** To answer Q3, we perform a sensitivity analysis by fixing the target environment (OOD-1 in the double pendulum task) and varying the simulation parameter space. In OOD-1, the OOD parameter is  $m_2 = 0.3$  while the range in  $\Omega$  is  $[1, 2]$ . Fig. 7 shows the results of reward achieved after adaptation for AdaptSim and the two Sys-ID baselines, as the range shifts further away from  $m_2 = 0.3$  to  $[1.1, 2.1]$ ,  $[1.2, 2.2]$ , and  $[1.3, 2.3]$ . Sys-ID performance degrades rapidly, while AdaptSim is more robust.

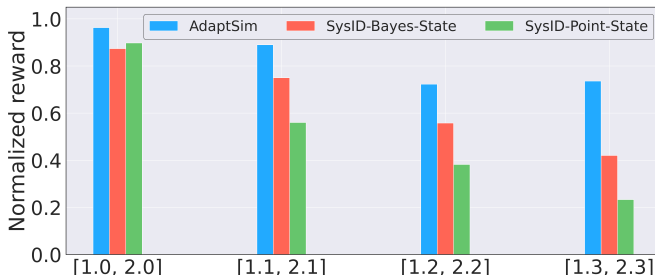


Fig. 7: Adaptation results for AdaptSim and Sys-ID baselines in OOD-1 setting of the double pendulum task, with different  $m_2$  ranges in  $\Omega$  while  $m_2 = 0.3$  in the target environment.

**Comparison of simulation parameter distributions found by AdaptSim vs. Sys-ID.** We expect that AdaptSim finds simulation settings that achieve better task performance while not necessarily minimizing the full dynamics discrepancies between simulation and reality. Fig. 8 shows the maximum possible task reward at all combinations of simulation parameters (after discretization) in OOD-1 setting of the double pendulum task, as well as the parameters found by AdaptSim vs. SysID-Bayes. SysID-Bayes finds parameters that are closer to the target in the parameter space, but for the specific task of swinging up the double pendulum, such parameters lead to inferior task reward compared to those found by AdaptSim.

Fig. 9 and Fig. 10 further demonstrate cases in the pushing and scooping tasks where SysID-Bayes under-performs

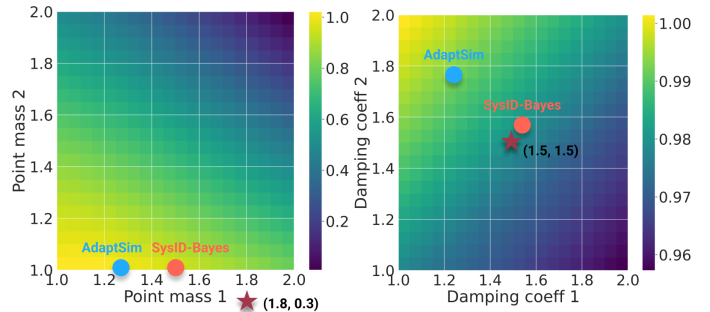


Fig. 8: Comparison of simulation parameters used after adaptation with AdaptSim and SysID-Bayes, in the OOD-1 setting of the double pendulum task. The two plots show the maximum possible normalized reward at each parameter setting. For each pair of point mass (left) or damping coefficient (right), we take the maximum over all possible pairs of the other two parameters. The target environment is defined with parameters  $(m_1=1.8, m_2=0.3, b_1=1.5, b_2=1.5)$  (dark red star). SysID-Bayes finds parameters closer to the target in the parameter space, but the task performance is worse.

AdaptSim and there are visible differences between simulation parameter distributions (showing mean only) found by the two approaches. In the pushing task, SysID-Bayes infers table and patch friction coefficients that are too low, and the trained task policy pushes the bottle with little speed. In the scooping task, interestingly, AdaptSim infers an ellipsoidal shape for the sliced cucumber despite it resembling a very thin cylinder, and the task policy achieves 60% success rate. Sys-ID infers a cylindrical shape but the task policy fails completely.

Fig. 11 demonstrates the dynamics mismatch between simulation and reality, which illustrates the pitfall of SysID approaches. We plot a set of bottle trajectories from randomly sampled simulation parameters from  $\Omega$  with a fixed robot action. We also plot the trajectories of Heavy bottle being pushed with the same action in reality. There are segments of real trajectories that are not well matched by the simulated ones, and a slight mismatch can lead to diverging final states (and hence different task rewards).

**Failure modes of AdaptSim.** We note that in some settings AdaptSim does not outperform baselines (e.g., OOD-4 in the pushing task and scooping up Brussels sprout in hardware). We attribute it to two plausible causes. First, AdaptSim’s task-

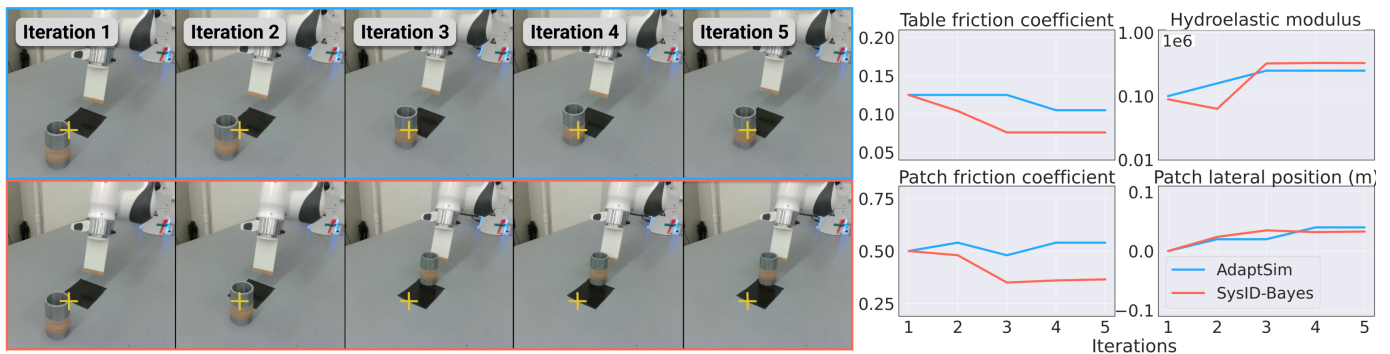


Fig. 9: Comparison of task performance of AdaptSim (top row) and SysID-Bayes (bottom row) over adaptation iterations when pushing Light bottle to a specific target location (yellow cross), as well as simulation parameter distribution (line plots showing the mean only) found by the two approaches. SysID-Bayes infers table and patch friction coefficients that are too low and the trained task policy pushes the bottle insufficient distance, while AdaptSim correctly learns to push the bottle faster and closer to the target, with inferred simulation parameters of higher task-relevance diverged from the SysID ones.

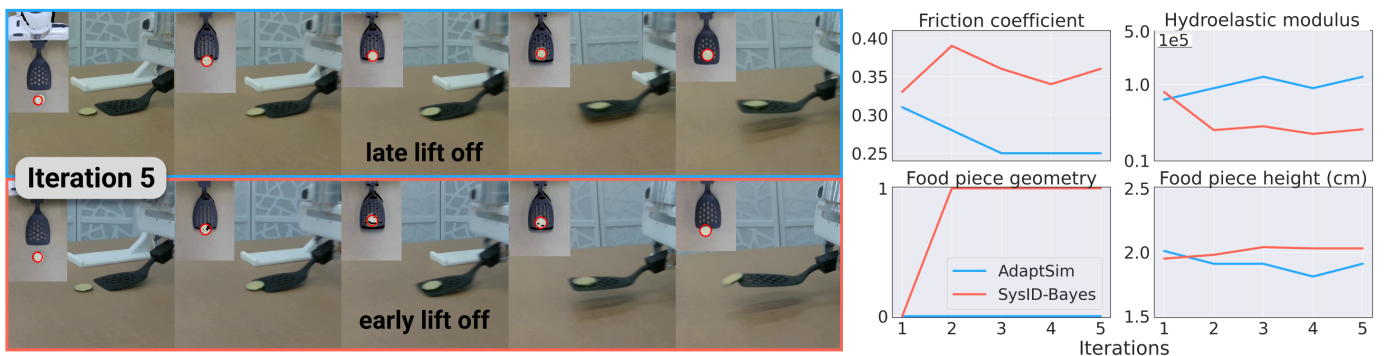


Fig. 10: Comparison of task performance of AdaptSim (top row) and SysID-Bayes (bottom row) at the end of adaptation when learning to scoop up the fake sliced cucumber, as well as simulation parameter distribution (line plots showing the mean only) found by the two approaches over iterations. The inset images show the top-down view of a RGB-D camera that tracks the food piece (tracked contours shown as red circles). With AdaptSim, the piece is successfully scooped up by lifting off the spatula relatively late; otherwise, the piece is first scooped up but then slips off the spatula. AdaptSim infers an ellipsoidal shape ( $g = 1$ , food piece geometry), while SysID-Bayes infers a cylindrical shape.

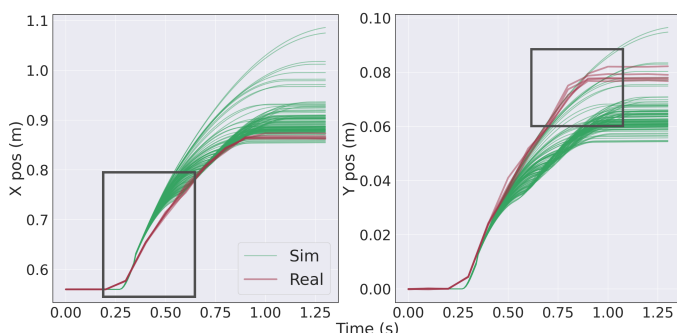


Fig. 11: Comparison of trajectories from the simulation domain (green, simulated with randomly sampled simulation parameter settings) and from Heavy bottle in reality (red), with the same robot action applied. The real dynamics can be OOD from simulation (black boxes) while the final position of the bottle can be WD.

driven adaptation training requires the trained task policy being (nearly) optimal on the corresponding simulation parameter distribution — while it can be solved exactly in the double pendulum task, the task policy training in the two manipulation tasks can be noisy. This may lead to sub-optimal task performance such as in OOD-1 setting of the scooping task.



Fig. 12: AdaptSim fails to synthesize a task policy for scooping up Brussels sprout. We consider such environment extremely OOD from the simulation domain.

Second, if the target environment is extremely OOD from the simulation domain, AdaptSim may not work as well. An example is to scoop up Brussels sprouts. Fig. 12 shows the sprout with highly irregular surface and high rigidity bounces on the spatula pad and rolls off from the other end; such behavior is not seen in simulation.

We believe the first issue can be mitigated by allowing more simulation budget for task policy training and better design of task policy re-use. The second issue can be addressed by designing the simulation parameter space  $\Omega$  to better cover possible real-world behavior.

**Comparison of simulation runtime.** Compared to Sys-ID baselines, AdaptSim requires significantly longer simulation

runtime for training the adaptation policy in Phase 1. For example: SysID-Bayes uses roughly 6 hours of simulation walltime to perform 10 iterations of adaptation in the scooping task while AdaptSim would take 36 hours for Phase 1, and 30 minutes for Phase 2 (i.e., 3 minutes per iteration), using the same computation setup. However, we re-use the same adaptation policy for different food pieces in the scooping task, which amortizes the simulation cost.

## VIII. CONCLUSION

In this work we present *AdaptSim*, a framework for efficiently adapting simulation-trained task policies to the real world. AdaptSim meta-learns how to adapt simulation parameter distributions for better performance in diverse simulated target environments, and then infers better distributions for training real-world task policies using a small amount of real data. The key insight behind our approach is that optimizing simulation parameters to match observed dynamics is often suboptimal for specific tasks in the presence of irreducible sim-to-real gap. Instead, we suggest finding simulation parameters that induce high quality behavior in the real world, regardless of how well they perfectly match the underlying physics of reality.

We believe our work opens up exciting research directions in leveraging powerful and expressive simulators for task-driven real-world policy learning. In future work, we aim to relax many of the design choices under practical considerations in this work, e.g., by using an adaptive step size and adaptive covariance for simulation parameter updates. Using differentiable simulation can speed up task policy training and help estimate the gradient of predicted task performance with respect to simulation parameters. We are also interested in examining the effect of under-parameterization and over-parameterization of the simulation ( $\Omega$ ) on best achievable task performance.

## ACKNOWLEDGMENTS

The authors were partially supported by the Toyota Research Institute (TRI), the NSF CAREER Award [#2044149], and the Office of Naval Research [N00014-23-1-2148, N00014-21-1-2803]. This article solely reflects the opinions and conclusions of its authors and NSF, ONR, TRI or any other Toyota entity. The authors would like to thank the Dynamics and Simulation team and Dexterous Manipulation team at TRI Robotics for technical support and guidance. We also thank Yimin Lin for helpful discussions.

## REFERENCES

- [1] Anurag Ajay, Maria Bauza, Jiajun Wu, Nima Fazeli, Joshua B Tenenbaum, Alberto Rodriguez, and Leslie P Kaelbling. [Combining physical simulators and object-based networks for control](#). In *Proceedings of the IEEE International Conference on Robotics and Automation (ICRA)*, 2019.
- [2] Ilge Akkaya, Marcin Andrychowicz, Maciek Chociej, Mateusz Litwin, Bob McGrew, Arthur Petron, Alex Paino, Matthias Plappert, Glenn Powell, Raphael Ribas, et al. [Solving rubik’s cube with a robot hand](#). *arXiv preprint arXiv:1910.07113*, 2019.
- [3] Adam Allevato, Elaine Schaefer Short, Mitch Pryor, and Andrea Thomaz. [Tunenet: One-shot residual tuning for system identification and sim-to-real robot task transfer](#). In *Proceedings of the Conference on Robot Learning (CoRL)*, 2020.
- [4] Rika Antonova, Fabio Ramos, Rafael Possas, and Dieter Fox. [BayesSimIG: Scalable Parameter Inference for Adaptive Domain Randomization with Isaac Gym](#). *arXiv preprint arXiv:2107.04527*, 2021.
- [5] Rika Antonova, Jingyun Yang, Priya Sundareshan, Dieter Fox, Fabio Ramos, and Jeannette Bohg. [A bayesian treatment of real-to-sim for deformable object manipulation](#). *IEEE Robotics and Automation Letters*, 7(3):5819–5826, 2022.
- [6] Alain Bensoussan. *Stochastic control of partially observable systems*. Cambridge University Press, 1992.
- [7] Yevgen Chebotar, Ankur Handa, Viktor Makoviychuk, Miles Macklin, Jan Issac, Nathan Ratliff, and Dieter Fox. [Closing the sim-to-real loop: Adapting simulation randomization with real world experience](#). In *Proceedings of the IEEE International Conference on Robotics and Automation (ICRA)*, 2019.
- [8] Yutian Chen, Matthew W Hoffman, Sergio Gómez Colmenarejo, Misha Denil, Timothy P Lillicrap, Matt Botvinick, and Nando Freitas. [Learning to learn without gradient descent by gradient descent](#). In *Proceedings of the International Conference on Machine Learning (ICML)*, 2017.
- [9] Cheng Chi, Benjamin Burchfiel, Eric Cousineau, Siyuan Feng, and Shuran Song. [Iterative residual policy: for goal-conditioned dynamic manipulation of deformable objects](#). In *Proceedings of Robotics: Science and Systems*, 2022.
- [10] Ben Evans, Abitha Thankaraj, and Lerrel Pinto. [Context is everything: Implicit identification for dynamics adaptation](#). In *Proceedings of the IEEE International Conference on Robotics and Automation (ICRA)*, 2022.
- [11] Justin Fu, Katie Luo, and Sergey Levine. [Learning robust rewards with adversarial inverse reinforcement learning](#). In *Proceedings of the International Conference on Learning Representations (ICLR)*, 2018.
- [12] Maxime Gautier and Wisama Khalil. [On the identification of the inertial parameters of robots](#). In *Proceedings of the IEEE Conference on Decision and Control (CDC)*, 1988.
- [13] Hugo Siqueira Gomes, Benjamin Léger, and Christian Gagné. [Meta learning black-box population-based optimizers](#). In *Proceedings of the International Conference on Learning Representations (ICLR)*, 2023.
- [14] Jennifer Grannen, Yilin Wu, Suneel Belkale, and Dorsa Sadigh. [Learning bimanual scooping policies for food acquisition](#). In *Proceedings of the Conference on Robot Learning (CoRL)*, 2022.
- [15] Shixiang Gu, Timothy Lillicrap, Ilya Sutskever, and

- Sergey Levine. [Continuous deep q-learning with model-based acceleration](#). In *Proceedings of the International Conference on Machine Learning (ICML)*, 2016.
- [16] Ankur Handa, Arthur Allshire, Viktor Makoviychuk, Aleksei Petrenko, Ritvik Singh, Jingzhou Liu, Denys Makoviichuk, Karl Van Wyk, Alexander Zhurkevich, Balakumar Sundaralingam, et al. [DeXTreme: Transfer of Agile In-hand Manipulation from Simulation to Reality](#). *arXiv preprint arXiv:2210.13702*, 2022.
- [17] Eric Heiden, Christopher E Denniston, David Millard, Fabio Ramos, and Gaurav S Sukhatme. [Probabilistic Inference of Simulation Parameters via Parallel Differentiable Simulation](#). In *Proceedings of the IEEE International Conference on Robotics and Automation (ICRA)*, 2022.
- [18] Kai-Chieh Hsu, Allen Z. Ren, Duy P Nguyen, Anirudha Majumdar, and Jaime F Fisac. [Sim-to-Lab-to-Real: Safe reinforcement learning with shielding and generalization guarantees](#). *Artificial Intelligence*, 314:103811, 2023.
- [19] Wanxin Jin and Michael Posa. [Task-Driven Hybrid Model Reduction for Dexterous Manipulation](#). *arXiv preprint arXiv:2211.16657*, 2022.
- [20] Lars Johannsmeier, Malkin Gerchow, and Sami Haddadin. [A framework for robot manipulation: Skill formalism, meta learning and adaptive control](#). In *Proceedings of the IEEE International Conference on Robotics and Automation (ICRA)*, 2019.
- [21] Pradeep K Khosla and Takeo Kanade. [Parameter identification of robot dynamics](#). In *Proceedings of the IEEE Conference on Decision and Control (CDC)*, 1985.
- [22] Ashish Kumar, Zipeng Fu, Deepak Pathak, and Jitendra Malik. [RMA: Rapid motor adaptation for legged robots](#). In *Proceedings of Robotics: Science and Systems*, 2021.
- [23] Joonho Lee, Jemin Hwangbo, Lorenz Wellhausen, Vladlen Koltun, and Marco Hutter. [Learning quadrupedal locomotion over challenging terrain](#). *Science Robotics*, 5(47):eabc5986, 2020.
- [24] Jacky Liang, Saumya Saxena, and Oliver Kroemer. [Learning active task-oriented exploration policies for bridging the sim-to-real gap](#). In *Proceedings of Robotics: Science and Systems*, 2020.
- [25] Vincent Lim, Huang Huang, Lawrence Yunliang Chen, Jonathan Wang, Jeffrey Ichnowski, Daniel Seita, Michael Laskey, and Ken Goldberg. [Planar robot casting with real2sim2real self-supervised learning](#). In *Proceedings of the IEEE International Conference on Robotics and Automation (ICRA)*, 2022.
- [26] Antonio Loquercio, Elia Kaufmann, René Ranftl, Alexey Dosovitskiy, Vladlen Koltun, and Davide Scaramuzza. [Deep drone racing: From simulation to reality with domain randomization](#). *IEEE Transactions on Robotics*, 36(1):1–14, 2019.
- [27] Gabriel B Margolis and Pulkit Agrawal. [Walk These Ways: Tuning Robot Control for Generalization with Multiplicity of Behavior](#). In *Proceedings of the Conference on Robot Learning (CoRL)*, 2022.
- [28] Joseph Masterjohn, Damrong Guoy, John Shepherd, and Alejandro Castro. [Velocity Level Approximation of Pressure Field Contact Patches](#). *IEEE Robotics and Automation Letters*, 7(4):11593–11600, 2022.
- [29] Bhairav Mehta, Manfred Diaz, Florian Golemo, Christopher J Pal, and Liam Paull. [Active domain randomization](#). In *Proceedings of the Conference on Robot Learning (CoRL)*, 2020.
- [30] Fabio Muratore, Christian Eilers, Michael Gienger, and Jan Peters. [Data-efficient domain randomization with bayesian optimization](#). *IEEE Robotics and Automation Letters*, 6(2):911–918, 2021.
- [31] Fabio Muratore, Fabio Ramos, Greg Turk, Wenhao Yu, Michael Gienger, and Jan Peters. [Robot learning from randomized simulations: A review](#). *Frontiers in Robotics and AI*, 9, 2022.
- [32] Anusha Nagabandi, Gregory Kahn, Ronald S Fearing, and Sergey Levine. [Neural network dynamics for model-based deep reinforcement learning with model-free fine-tuning](#). In *Proceedings of the IEEE International Conference on Robotics and Automation (ICRA)*, 2018.
- [33] Xue Bin Peng, Marcin Andrychowicz, Wojciech Zaremba, and Pieter Abbeel. [Sim-to-real transfer of robotic control with dynamics randomization](#). In *Proceedings of the IEEE International Conference on Robotics and Automation (ICRA)*, 2018.
- [34] Fabio Ramos, Rafael Carvalhaes Possas, and Dieter Fox. [Bayessim: adaptive domain randomization via probabilistic inference for robotics simulators](#). In *Proceedings of Robotics: Science and Systems*, 2019.
- [35] Allen Z. Ren and Anirudha Majumdar. [Distributionally robust policy learning via adversarial environment generation](#). *IEEE Robotics and Automation Letters*, 7(2):1379–1386, 2022.
- [36] Allen Z. Ren, Bharat Govil, Tsung-Yen Yang, Karthik Narasimhan, and Anirudha Majumdar. [Leveraging Language for Accelerated Learning of Tool Manipulation](#). In *Proceedings of the Conference on Robot Learning (CoRL)*, 2022.
- [37] Nataniel Ruiz, Samuel Schuler, and Manmohan Chandraker. [Learning to simulate](#). In *Proceedings of the International Conference on Learning Representations (ICLR)*, 2019.
- [38] Fereshteh Sadeghi and Sergey Levine. [Cad2rl: Real single-image flight without a single real image](#). In *Proceedings of Robotics: Science and Systems*, 2017.
- [39] Daniel Seita, Yufei Wang, Sarthak J Shetty, Edward Yao Li, Zackory Erickson, and David Held. [ToolFlowNet: Robotic Manipulation with Tools via Predicting Tool Flow from Point Clouds](#). In *Proceedings of the Conference on Robot Learning (CoRL)*, 2022.
- [40] Jan Swevers, Chris Ganseman, D Bilgin Tukul, Joris De Schutter, and Hendrik Van Brussel. [Optimal robot excitation and identification](#). *IEEE Transactions on Robotics and Automation*, 13(5):730–740, 1997.
- [41] Arash Tavakoli, Fabio Pardo, and Petar Kormushev.

- Action Branching Architectures for Deep Reinforcement Learning. In *Proceedings of the AAAI Conference on Artificial Intelligence*, 2018.
- [42] Russ Tedrake. *Underactuated Robotics*. 2023. URL <https://underactuated.csail.mit.edu>.
- [43] Russ Tedrake and the Drake Development Team. *Drake: Model-based design and verification for robotics*, 2019. URL <https://drake.mit.edu>.
- [44] Josh Tobin, Rachel Fong, Alex Ray, Jonas Schneider, Wojciech Zaremba, and Pieter Abbeel. [Domain randomization for transferring deep neural networks from simulation to the real world](#). In *Proceedings of the IEEE/RSJ International Conference on Intelligent Robots and Systems (IROS)*, 2017.
- [45] Hado Van Hasselt, Arthur Guez, and David Silver. [Deep reinforcement learning with double q-learning](#). In *Proceedings of the AAAI conference on artificial intelligence*, 2016.
- [46] Michael Volpp, Lukas P Fröhlich, Kirsten Fischer, Andreas Doerr, Stefan Falkner, Frank Hutter, and Christian Daniel. [Meta-learning acquisition functions for transfer learning in bayesian optimization](#). In *Proceedings of the International Conference on Learning Representations (ICLR)*, 2020.
- [47] Quan Vuong, Sharad Vikram, Hao Su, Sicun Gao, and Henrik I Christensen. [How to pick the domain randomization parameters for sim-to-real transfer of reinforcement learning policies?](#) *arXiv preprint arXiv:1903.11774*, 2019.
- [48] Martin Wistuba, Nicolas Schilling, and Lars Schmidt-Thieme. [Scalable gaussian process-based transfer surrogates for hyperparameter optimization](#). *Machine Learning*, 107(1):43–78, 2018.
- [49] Wenhao Yu, Jie Tan, C Karen Liu, and Greg Turk. [Preparing for the unknown: Learning a universal policy with online system identification](#). In *Proceedings of Robotics: Science and Systems*, 2017.
- [50] Wenhao Yu, C Karen Liu, and Greg Turk. [Policy transfer with strategy optimization](#). In *Proceedings of the International Conference on Learning Representations (ICLR)*, 2018.
- [51] Andy Zeng, Shuran Song, Johnny Lee, Alberto Rodriguez, and Thomas Funkhouser. [Tossingbot: Learning to throw arbitrary objects with residual physics](#). *IEEE Transactions on Robotics*, 36(4):1307–1319, 2020.

## APPENDIX A

### ADDITIONAL DETAILS OF ADAPTATION POLICIES

**Hyperparameters.** Table A1 shows the hyperparameters used for the adaptation policy training in Phase 1, including those defining the heuristics for re-using task policies among simulation parameter distributions. We generally use smaller adaptation step  $\delta$  for smaller dimensional  $\Omega$ .

Parameter	Task		
	Pendulum	Pushing	Scoping
Total adaptation steps, $K$	1e4	1e4	1e4
Adaptation horizon, $I$	10	8	8
Adaptation step size, $\delta$	0.10	0.15	0.15
Adaptation discount factor, $\gamma$	0.9	0.9	0.9
Sparse reward threshold, $\bar{R}$	0.95	0.8	0.5
Task policy reuse threshold, $\bar{D}$	-	0.16	0.16
Task policy max budget, $M_{\max}$	-	3e4	4e3
Task policy budget discount, $\alpha$	-	0.9	0.9
Task policy init budget, $M$	-	1e4	1.2e3

TABLE A1: Hyperparameters used in adaptation policy training for the three tasks.

**Trajectory observations.** We detail the trajectory observation (as input to the adaptation policy) used in the three tasks.

- Pendulum task: each trial is 2.5 seconds long, and we use 12 evenly spaced points along the trajectories of the two joints, and thus each trajectory is 24 dimensional. For AdaptSim-State, SysID-Bayes-State, and SysID-Bayes-Point, again 12 points are used but sampled from the last 0.5 second only. One trajectory is used at each adaptation iteration — the trajectory input to the adaptation policy is 24 dimensional.
- Pushing task: each trial is 1.3 seconds long, and we use 6 evenly spaced points along the X-Y trajectory of the bottle, and thus each trajectory is also 12 dimensional. For AdaptSim-State, SysID-Bayes-State, and SysID-Bayes-Point, only the final X-Y position of the bottle is used. Two trajectories are used at each adaptation iteration — the trajectory input to the adaptation policy is 24 dimensional.
- Scoping task: each trial is 1 second long, and we use X-Y position of the food piece at the time step  $[0, 0.2, 0.3, 0.4, 0.5, 0.6, 0.8, 1.0]$ s (more sampling around the initial contact between the spatula and the piece), and thus each trajectory is 16 dimensional. Two trajectories are used at each adaptation iteration — the trajectory input to the adaptation policy is 32 dimensional.

In real experiments, we track the bottle position in the pushing task using 3D point cloud information from a Azure Kinect RGB-D camera, which we find accurate. In the scoping task, the food pieces are too small and thin to be reliably tracked with point cloud, and thus we resort to extracting the contours from the RGB image and then finding the corresponding depth values at the same pixels in the depth image. During fast contact there can be motion blur around the food piece, and thus we add Gaussian noise with 0.2cm mean for X position

and zero mean for Y position, and 0.2cm covariance for both, to the points in the ground-truth trajectories in simulation. We use positive mean in X since the motion blur tends to occur in the forward direction.

## APPENDIX B

### ADDITIONAL DETAILS OF THE TASK SETUP AND TASK POLICIES

#### A. *Dynamic pushing of a bottle*

**Trajectory parameterization.** Here we detail the trajectory of the end-effector pusher designed for the task (Fig. A3). The trajectory is parameterized with two parameters: (1) planar pushing angle, which is the yaw orientation of the pusher relative to the forward direction that controls the direction of the bottle being pushed, and (2) forward speed (of the end-effector), in the direction specified by the pushing angle. The pushing angle varies between  $-0.3\text{rad}$  and  $0.3\text{rad}$ , and the forward speed varies between  $0.4\text{m/s}$  and  $0.8\text{m/s}$ . We find  $0.8\text{m/s}$  roughly the upper speed limit of the Franka Panda arm used. The pusher also pitches upwards during the motion and the speed is fixed to  $0.8\text{rad/s}$ . We design such trajectories to maximize the pushing distance at the hardware limit.

**Initial and goal states.** The bottle is placed at the fixed location ( $x=0.56\text{m}$ ,  $y=0$ , relative to the arm base) on the table before the trial starts. The goal location is sampled from a region where the X location is between  $0.7$  and  $1.0\text{m}$  and Y location is at most  $10$  degrees off from the centerline (Fig. A3 top-right). The patch, a  $10\text{cm}$  by  $10\text{cm}$  square, is placed at  $x = 0.75\text{m}$  with its center (lateral position is varied as one of the simulation parameter).

**Task policy parameterization.** The task policy is parameterized using a Normalized Advantage Function (NAF) [15] that allows efficient Q Learning with continuous action output by restricting the Q value as a quadratic function of the action, and thus the action that maximizes the Q value can be found exactly without sampling. In this task, it maps the desired 2D goal location of the bottle to the two action parameters, planar pushing angle and forward speed. The policy is open-loop — the actions are determined before the trial starts and there is no feedback using camera observations.

**Hardware setup.** A 3D-printed, plate-like pusher is mounted at the end-effector instead of the parallel-jaw gripper in both simulation and reality. We also wrap elastic rubber bands around the bottom of the pusher and contact regions of the bottle to induce more elastic collision, which we find increases the sliding distance of the bottle.

#### B. *Dynamic scooping of food pieces*

**Trajectory parameterization.** Here we detail the trajectory of the end-effector with the spatula designed for the task (Fig. A4). The end-effector velocity trajectory is generated using cubic spline with values clamped at five timesteps. The trajectory only varies in the X and pitch direction (in the world frame), while remaining zero in the other directions. The only value defining the trajectory that the task policy learns is the pitch rate, which is the pitch speed at the time  $t=0.25\text{s}$  and varies between  $-0.2\text{rad/s}$  and  $0.2\text{rad/s}$ . A positive pitch rate means the spatula lifting off the table late, while a negative one means lifting off early (see the effects in Fig. 10). The other two values that the task policy outputs are the initial pitch angle of the spatula from the table (varying from  $2$  to  $10$  degrees), and the initial distance between the spatula and the food piece (varying between  $0.5\text{cm}$  to  $2\text{cm}$ ). Generally a higher initial pitch angle can help scoop under food pieces with flat bottom, and a smaller angle helps scoop under ellipsoidal shapes. We design such trajectories after extensive testing with food pieces of diverse geometric shapes and physical properties in both simulation and reality.

**Initial states.** The food piece is randomly placed in a box area of  $8\times 6\text{cm}$  in front of the spatula; the initial distance is relative to the initial food piece location.

**Task policy parameterization.** The task policy is parameterized using a NAF again. In this task, it maps the initial 2D position of the food piece to the three action parameters: pitch rate, initial pitch angle, and initial distance.

**Hardware setup.** We use the commercially available OXO Nylon Square Turner<sup>2</sup> as the spatula used for scooping. It has a relatively thin edge (about  $1.2\text{mm}$ ) that helps scoop under thin pieces. A box-like, 3D-printed adapter with high-friction tape is mounted on the handle to help the parallel-jaw gripper grasp the spatula firmly. The exact 3D model of the spatula with the adapter is designed and used in the Drake simulator; the deformation effect as it bends against the table is not modeled in simulation.

## APPENDIX C

### ADDITIONAL DETAILS OF EXPERIMENTS

#### A. *Simulated adaptation*

Table A2 shows the simulation parameters used in different simulated target environments for the three tasks (results shown in Table IV).

#### B. *Real adaptation*

In Fig. A5 and Fig. A6 we demonstrate additional visualizations of the pushing and scooping results with AdaptSim.

<sup>2</sup>link: <https://www.amazon.com/OXO-11107900LOW-Grips-Square-Turner/dp/B003L0OOSU>

Task	Parameter	Setting					Range
		WD	OOD-1	OOD-2	OOD-3	OOD-4	
Pendulum	$m_1$	1.8	1.8	<b>0.5</b>	1.2	<b>0.4</b>	[1, 2]
	$m_2$	1.2	<b>0.3</b>	1.8	1.8	<b>2.6</b>	[1, 2]
	$b_1$	1.5	1.5	1.5	<b>10.0</b>	1.0	[1, 2]
	$b_2$	1.5	1.5	1.5	<b>10.0</b>	2.0	[1, 2]
Pushing	$\mu$	0.1	<b>0.25</b>	0.05	0.15	<b>0.30</b>	[0.05, 0.2]
	$e$	1e5	5e4	1e5	<b>5e6</b>	1e5	[1e4, 1e6]
	$\mu_p$	0.6	<b>0.1</b>	<b>0.9</b>	<b>0.1</b>	<b>0.15</b>	[0.2, 0.8]
	$y_p$	0.05	-0.1	0.05	<b>-0.15</b>	0.1	[-0.1, 0.1]
Scooping	$\mu$	0.30	<b>0.45</b>	<b>0.20</b>	0.30	0.40	[0.25, 0.4]
	$e$	5e4	1e4	5e4	<b>1e6</b>	1e5	[1e4, 5e5]
	$g$	1	0	1	0	<b>2</b>	{0, 1}
	$h$	2.0	<b>1.4</b>	2.2	<b>2.8</b>	1.9	[1.5, 2.5]

TABLE A2: Simulation parameters used in different simulated target environments for the three tasks. OOD parameters (outside the range used in adaptation policy training) are bolded. For  $g$  in the scooping task, 0 stands for ellipsoid, 1 for cylinder, and 2 for box.

### C. Additional studies

**Trade-off between real data budget and task performance convergence.** In Sec. IV-C we introduce  $N$ , the number of initial simulation parameter distributions that are sampled at the beginning of Phase 2 and then adapt independently. There is a trade-off between the real data budget (linear to  $N$ ) and convergence of task performance. Adapting more simulation parameter distributions simultaneously can potentially help the task performance converge faster but also require more real data. Fig. A1 shows the effect with the Light bottle in the pushing task. We vary  $N$  from 1 to 4 — each simulation parameter distribution takes 2 trajectories at each iteration.  $N = 1$  shows slow and also worse asymptotic convergence, which shows that the parameter distribution can be trapped in a low-reward regime.  $N = 2$  performs the best with fastest convergence in terms of number of real trajectories used. Using higher  $N$  shows slower convergence. Note that the convergence also depends on the dimension of the simulation parameter space  $\Omega$  — we expect  $N > 2$  is needed for the best convergence rate once the dimension increases from 4 used in the pushing task.

**Sensitivity analysis on adaptation step size.** Adaption step size  $\delta$  can affect the task performance convergence too —  $\delta$  being too low can cause slow convergence, while  $\delta$  being too high can prevent convergence since the simulation parameter distribution can “overshoot” the optimal one by a large margin. Fig. A2 shows the effect of adaptation step size ranging from 0.05 to 0.20 in OOD-1 setting of the double pendulum task.  $\delta = 0.10$  performs the best while  $\delta = 0.05$  shows slower convergence.  $\delta = 0.15$  also achieves similar asymptotic performance but the reward is less unstable during adaptation, while with  $\delta = 0.20$  the reward does not converge at all.

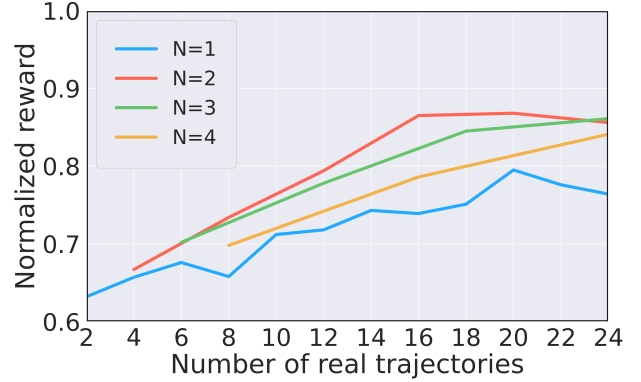


Fig. A1: Task performance convergence with respect to the number of real trajectories used with varying  $N$ , the number of simulation parameter distributions adapting simultaneously in Phase 2 with the Light bottle in the pushing task.

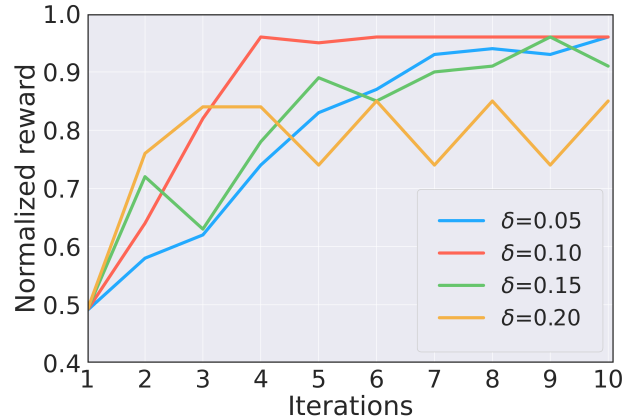


Fig. A2: Normalized reward at each adaptation iteration using different adaptation step size  $\delta$ , in OOD-1 setting of the pendulum task.

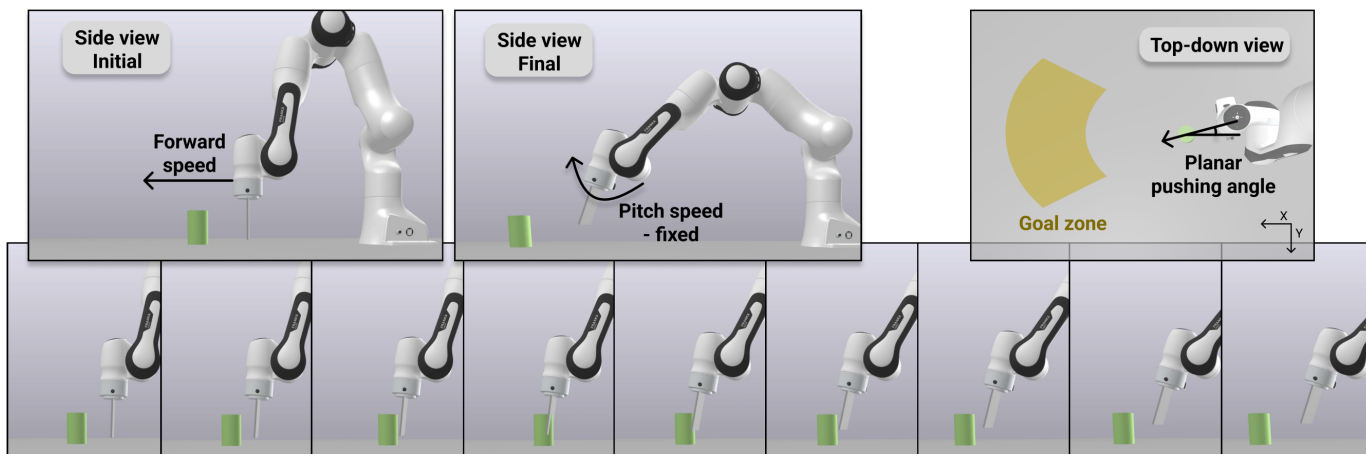


Fig. A3: Visualization of the pushing trajectory and goal locations in the Drake simulator. There are two action parameters: (1) forward speed (of the end-effector) and (2) planar pushing angle (*i.e.*, yaw orientation of the end-effector). The patch is not visualized.

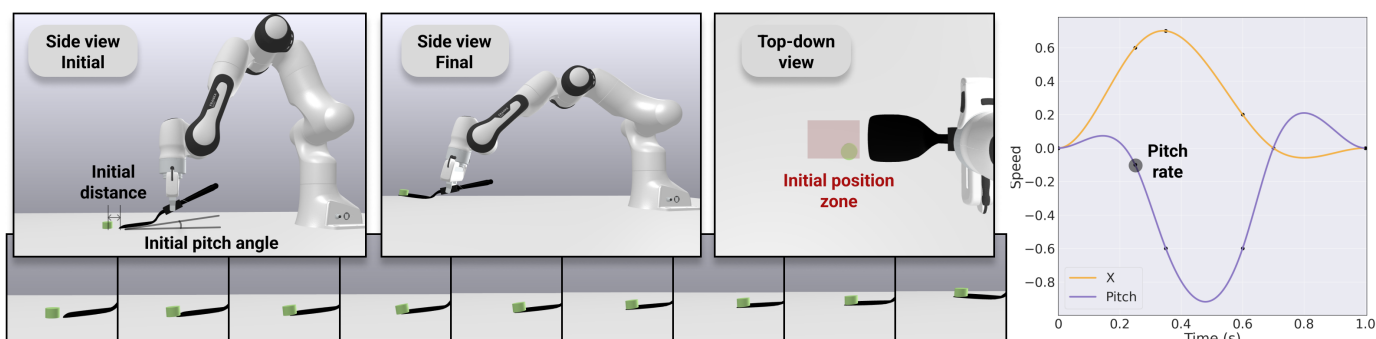


Fig. A4: Visualization of the scooping trajectory and initial positions of the food piece in the Drake simulator. There are three action parameters: (1) initial distance (between the spatula and food piece), (2) initial pitch angle (of the spatula from the table), and (3) pitch rate (of the end-effector at time step  $t = 0.25$ ).

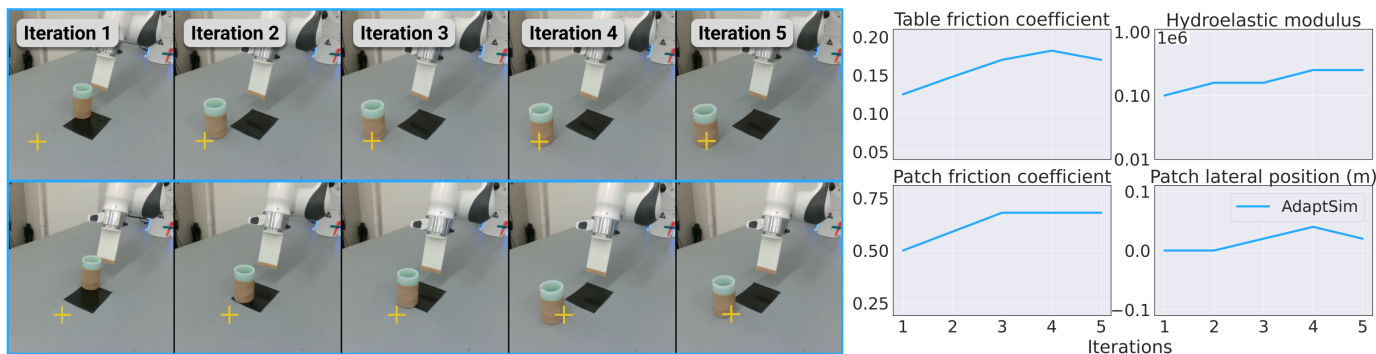


Fig. A5: Adaptation results of the pushing task with two different target locations (yellow cross, top and bottom rows) over iterations. The right figure shows the inferred simulation parameter distribution (mean only).

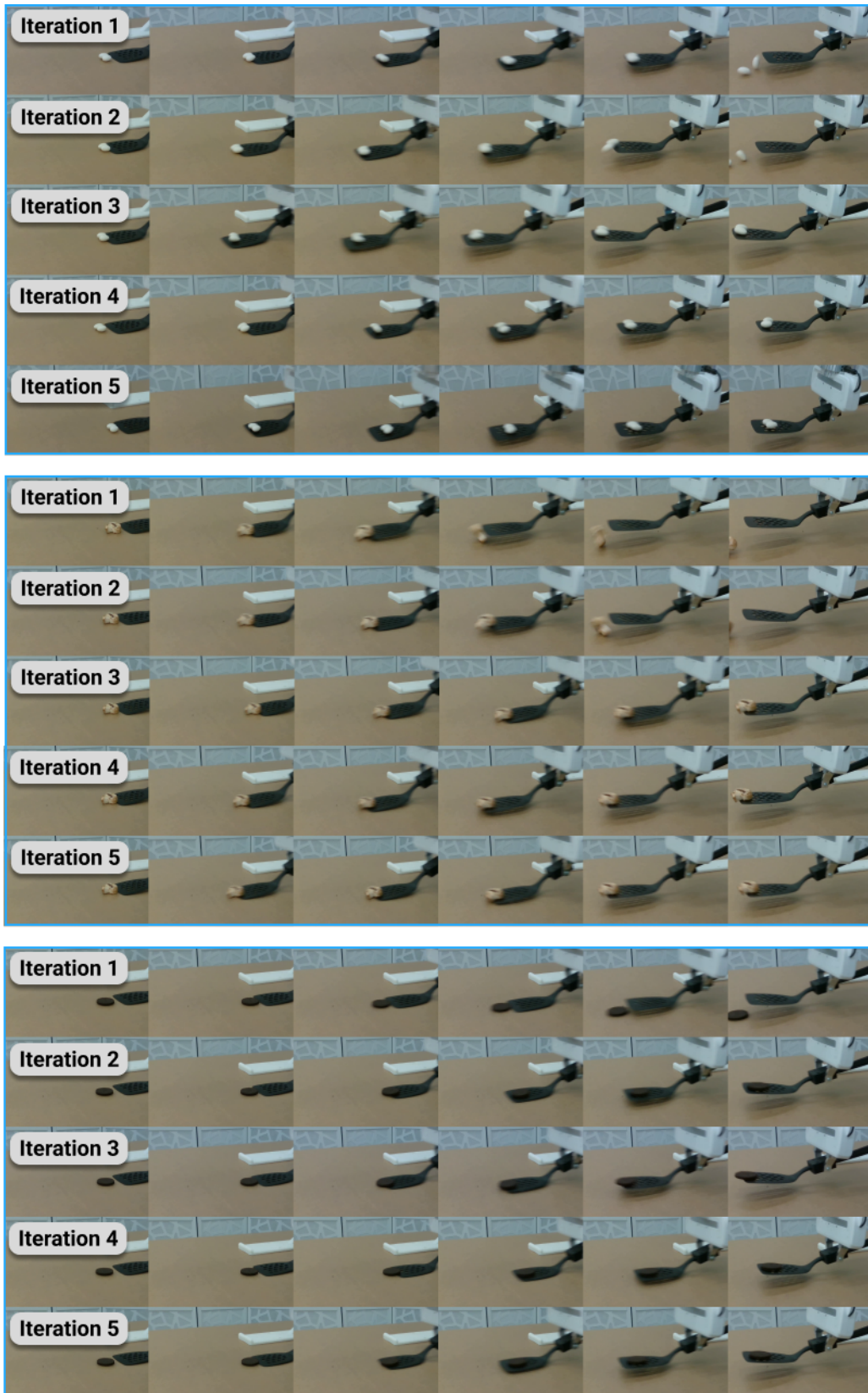


Fig. A6: Adaptation results of scooping up (top) chocolate raisins, (middle) mushroom slice, and (bottom) Oreo cookie with AdaptSim.